Published online 12 August 2020 *Nucleic Acids Research, 2020, Vol. 48, No. 17* ***9649–9659***
doi: 10.1093/nar/gkaa648

Conformational flexibility and oligomerization of BRCA2 regions induced by RAD51 interaction

Arshdeep Sidhu[1,2], Małgorzata Grosbart[1], Humberto Sánchez[3], Bram Verhagen[1], Nick L.L. van der Zon[1], Dejan Ristić[1], Sarah E. van Rossum-Fikkert[1] and Claire Wyman [1,2,*]

[1]Department of Molecular Genetics, Erasmus University Medical Center, 3000 CA Rotterdam, The Netherlands, [2]Department of Radiation Oncology and Cancer Genomics Center, Erasmus University Medical Center, 3000 CA Rotterdam, The Netherlands and [3]Department of Bionanoscience, Kavli Institute of Nanoscience, Faculty of Applied Sciences, Delft University of Technology, 2628 CJ Delft, The Netherlands

Received November 07, 2019; Revised July 15, 2020; Editorial Decision July 16, 2020; Accepted August 07, 2020

ABSTRACT

BRCA2 is a key breast cancer associated protein that is predicted to have interspersed regions of intrinsic disorder. Intrinsic disorder coupled with large size likely allows BRCA2 to sample a broad range of conformational space. We expect that the resulting dynamic arrangements of BRCA2 domains are a functionally important aspect of its role in homologous recombination DNA repair. To determine the architectural organization and the associated conformational landscape of BRCA2, we used scanning force microscopy based single molecule analyses to map the flexible regions of the protein and characterize which regions influence oligomerization. We show that the N- and the C-terminal regions are the main flexible regions. Both of these regions also influence BRCA2 oligomerization and interaction with RAD51. In the central Brc repeat region, Brc 1–4 and Brc 5–8 contribute synergistically to BRCA2 interaction with RAD51. We also analysed several single amino acid changes that are potentially clinically relevant and found one, the variant of F1524V, which disrupts key interactions and alters the conformational landscape of the protein. We describe the overall conformation spectrum of BRCA2, which suggests that dynamic structural transitions are key features of its biological function, maintaining genomic stability.

INTRODUCTION

Almost 80% of the proteins associated with human cancer are predicted to have intrinsically disordered regions (IDRs) of >30 amino-acids (1). Despite their ubiquity, the precise functional contribution of intrinsic disorder in these proteins has not been determined. IDRs participate in weak and transient but specific interactions facilitated by a conformational repertoire (2). Therefore, to understand the functional spectrum of such proteins it is important to map and define their conformational landscape.

BRCA2 is an essential protein with a well-defined role in the error-free repair of double-strand DNA breaks by homologous recombination repair (3,4). The best elucidated function of BRCA2 is to deliver the DNA strand exchange protein RAD51 to the site of DNA damage to facilitate repair (5,6). BRCA2 interacts with RAD51 primarily *via* the Brc repeat region that forms the middle one-third of the protein (Figure 1). The eight Brc repeats can each bind RAD51 and are reported to function in a modular fashion with different roles for Brc 1–4 and Brc 5–8. The two modules have been reported to have different affinities for RAD51, ranging between 1–2 μM (Brc 1, 2, 4) and 100–200 μM (Brc 6, 7 and 8) (7). The isolated modules are biochemically distinct with respect to the RAD51 forms they bind (monomers or filament polymers), their differential inhibition of DNA-dependent ATPase activity of RAD51, and their effects on RAD51-mediated DNA strand exchange *in vitro* (7–13). Each Brc repeat comprise about 35 aa including highly conserved tetra amino acid motifs of FxxA and LFxD/E, which are crucial for BRCA2–RAD51 interaction (10,14). This interaction is structurally well characterized in these isolated regions and assumed to represent the interaction in the full-length protein. In crystal structure of Brc 4 and RecA-homology domain of RAD51, residues F1524 to V1532 in Brc 4 form a β-hairpin with the F1524 being buried in a hydrophobic pocket formed by RAD51 (9). BRCA2 is also reported to interact with RAD51 through the C-terminal region, where phosphorylation of BRCA2 S3291 by cyclin-dependent kinases regulates RAD51 interaction and recombinase activity in the cell-cycle (15,16).

*To whom correspondence should be addressed. Tel: +31 10 704 4337; Fax: +31 10 704 4743; Email: c.wyman@erasmusmc.nl
Present address: Arshdeep Sidhu, Division of Molecular Biology and Cancer, Nitte University Centre for Science Education and Research, Nitte (Deemed to be University), Mangalore-575018, India.

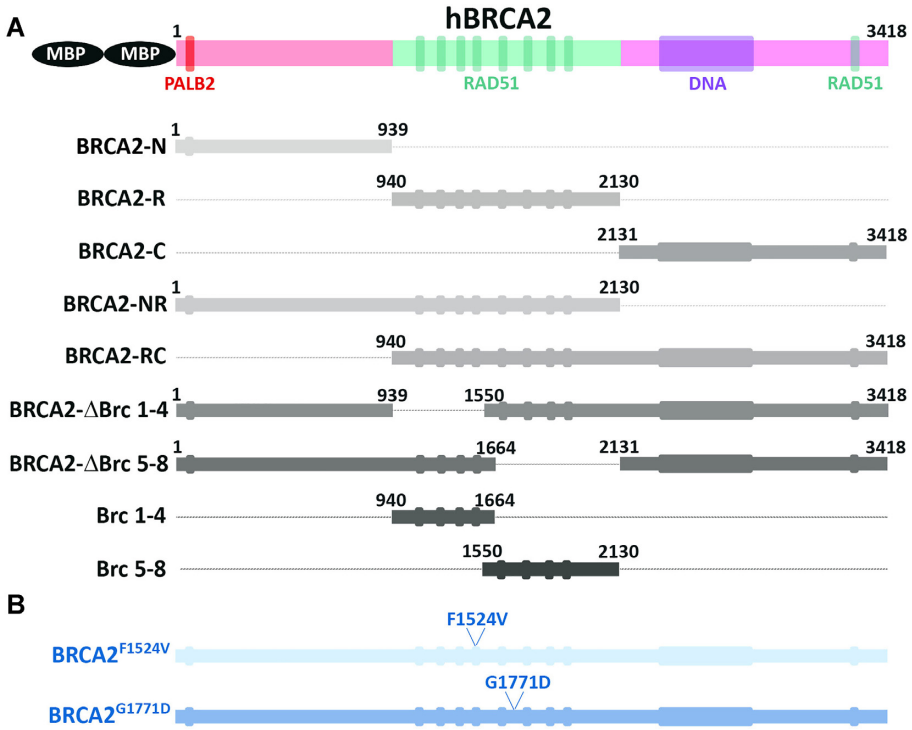

Figure 1. Schematic overview of the BRCA2 regions studied. (**A**) Different regions of fl-BRCA2 produced for this study. (**B**) Variants of unknown clinical significance produced for this study.

BRCA2 is predicted to have multiple stretches of intrinsic disorder interspersed along its 3418 amino acids (17). Some regions of the protein have defined structures, at least in complex with binding partners. The N-terminal aa 21–39, Brc 4 (aa 1517–1551) and the C-terminal region (mouse aa 2378–3114) have been crystallized in complex with parts of their binding partners, PALB2, RAD51 and DSS1 + single-stranded DNA, respectively. The crystal structure of the N-terminal region and Brc 4 adopts short stretches of α-helix and β-hairpin (9,18). The C-terminus folds in distinct domains; the helical domain (aa 2481–2668), the oligonucleotide binding domains (aa 2670–3185) and the tower domain (aa 2838–2962) (19). Although providing detailed structures for these regions of BRCA2, the isolated structures do not indicate how these regions are arranged in the full-length protein. Two major challenges in studying full-length BRCA2 (fl-BRCA2) are its size and abundant IDRs.

IDRs are typically associated with structural variability or flexibility, which is incompatible with methods that require a sample with uniform molecular structure (X-ray, NMR, EM reconstruction). In contrast, quantifying the distribution of forms in a conformational ensemble can provide unique insight into flexibility and the influence of protein-protein and protein–DNA interactions (17,20–25). IDRs allow protein molecules to act as dynamic conformational switches, sensitive to interaction with other proteins, environmental changes and post-translational modifications (2,26). We have previously characterized the conformational variability of fl-BRCA2 by single molecule scanning force microscopy (SFM) imaging (17). BRCA2 is observed to be a mixture of multimeric forms which were extended and apparently flexible molecules, or compact and globular, depending on the temperature of incubation and presence of binding partners. BRCA2 appears as a flexible molecule that switched conformation in response to temperature change from 37 to 0°C. Incubation of BRCA2 with RAD51 results in a compact elongated conformation, which can include multiple BRCA2 and RAD51 molecules per complex (17). Major changes in oligomerization of fl-BRCA2, from large oligomers to monomers, have also been reported by Le *et al.* on complexation with DSS1 and ssDNA (25). Thereby, highlighting the diverse conformational landscape of BRCA2 in protein-protein and protein–DNA interactions.

Here, we probe the contribution of different regions of BRCA2 to its conformational landscape by SFM. The N- and the C-terminal regions of BRCA2 are the most variable in structure, presumably due to flexibility. The central region including the Brc repeats appears to be involved in oligomerization, both self-association, BRCA2–BRCA2, and in BRCA2–RAD51 complexes. In agreement with previous studies, we show that in isolation the two Brc modules (1–4 and 5–8) are biochemically distinct. However, in the context of the whole protein the two modules contribute synergistically to the conformational landscape. We similarly analysed the architectural effects of two clinically relevant missense variants of the Brc region in detail, F1524V and G1771D. The single amino acid change F1524V in Brc 4 had a dramatic effect on BRCA2 conformational landscape and interaction with RAD51. These results highlight the importance of knowledge on the conformational distri-

bution of disordered proteins to identify factors that can affect their conformation and function.

MATERIALS AND METHODS

Protein expression and purification

Regions of BRCA2 (N region, R region, C region, NR region, RC region, BRCA2 ΔBrc 1–4, BRCA2 ΔBrc 5–8, Brc 1–4 and Brc 5–8), with two tandem N-terminal maltose binding protein (MBP) tag, and BRCA2 variants of unknown significance ($BRCA2^{F1524V}$, $BRCA2^{G1771D}$) were made by Q5® site directed mutagenesis (NEB) (Figure 1) (Plasmid for fl-BRCA2 gene was kindly gifted by S. Kowalczykowski). Positive clones for each variant were sequence verified. Proteins for temperature studies were purified according to protocol as described elsewhere (3), from plate cultures. For other studies, purified plasmids were transfected with 10% (v/v) transfection solution in 293T HEK cells, adapted for suspension culture, in FreeStyle™ 293 Expression Medium (Gibco) at approximately 10^6 cells/ml. Transfection solution was prepared by adding 1 μg/ml purified DNA and 2 μg/ml linear PEI in Serum-Free Hybridoma Media (Gibco®) supplemented with 1% FCS. Transfection solution was incubated for 20 min at room temperature and added to 500 ml or 1 l of HEK cell suspension growing at 37°C with shaking at 250 rpm. Except for cell cultures with the BRCA2 ΔBrc 1–4 construct, which showed highest number of cells 24 h post transfection, cells with all other constructs were harvested after 48 h, at a cell count of about 2×10^6 cells/ml, by centrifugation at 8000 × g at 4°C for 15 min. The cell pellet was resuspended in 10 ml ice cold PBS and frozen in liquid nitrogen. Next, cells were lysed in 200 ml lysis buffer (50 mM HEPES pH 7.5, 250 mM NaCl, 1% NP-40, 1 mM ATP, 3 mM $MgCl_2$, 1 mM Pefabloc SC [Merck], two tablets EDTA free protease inhibitor [Roche], 1 mM DTT) for 15 min at 4°C with shaking. The lysate was centrifuged at 10 000 × g at 4°C for 15 min. The supernatant was incubated overnight with 6 ml Amylose resin (NEB) pre-equilibrated in wash buffer (50 mM HEPES pH 7.5, 250 mM NaCl, 0.5 mM EDTA and 1 mM DTT). The next day, the beads were washed three times with wash buffer by centrifugation at 2000 × g at 4°C for 5 min and aspiration of the supernatant. The washed resin was incubated with elution buffer (50 mM maltose, 50 mM HEPES pH 8.2, 250 mM NaCl, 0.5 mM EDTA, 10% glycerol, 1 mM DTT, 1 mM Pefabloc SC) for 15 min at 4°C on a rolling platform. The eluate was collected by passing the slurry through a disposable BioRad column at 4°C. The eluate was loaded on a 1 ml HiTrap Q column (GE) using Q low buffer (50 mM HEPES pH 8.2, 250 mM NaCl, 0.5 mM EDTA, 10% glycerol, 1 mM DTT, 1 mM PMSF) and eluted with Q high buffer (50 mM HEPES pH 8.2, 1 M NaCl, 0.5 mM EDTA, 10% glycerol, 1 mM DTT, 1 mM PMSF). Fractions with proteins were aliquoted into single use aliquots, which were then snap frozen in liquid nitrogen and were stored at −80°C. Yield of protein purification, estimated by CBR-250 stained PAGE gels with BSA standards, was between 2 and 4 μg per preparation for all the regions (Supplementary Figure S1).

Purification at various steps was assessed by western blot using anti-BRCA2 antibodies. For N region, BRCA2 ΔBrc 5–8 and $BRCA2^{G1771D}$, rabbit polyclonal anti-BRCA2 (1:1000) (3675-Biovision) was used as the primary antibody followed by donkey anti-rabbit HRP (1:2500) (Jackson ImmunoResearch) as the secondary antibody. For R, NR, RC, BRCA2 ΔBrc 1–4, $BRCA2^{F1524V}$, mouse monoclonal anti-BRCA2, epitope aa 1651–1821 (1:500) (OP95-Calbiochem®) was used as the primary antibody and sheep anti-mouse HRP (1:2000) (Jackson ImmunoResearch) as the secondary antibody. For C, rabbit polyclonal anti-BRCA2, epitope aa 3245–3418 (1:500) (CA1033-Calbiochem®) was used as the primary antibody followed by donkey anti-rabbit HRP (1:2500) (Jackson ImmunoResearch) as the secondary antibody. For Brc 1–4, Brc 5–8, rabbit polyclonal anti-maltose binding protein (1:2000) (ab9084-abcam) was used as the primary antibody and donkey anti-rabbit HRP (1:2500) (Jackson ImmunoResearch) as the secondary antibody (Supplementary Figure S2).

Untagged human RAD51 was expressed and purified as described (21).

SFM sample preparation, imaging and analyses

Flexibility of BRCA2 regions. Aliquots of BRCA2 regions were thawed and diluted four-fold in 10 mM HEPES pH 8.2 buffer to prepare a reaction of 10 nM BRCA2 variant in 22 mM HEPES pH 8.2, 112 mM NaCl, 0.125 mM EDTA, 2.5% glycerol, 0.25 mM DTT. Samples were incubated at 37°C or 0°C (on ice) for 30 min without shaking.

BRCA2 variants–RAD51 interaction. For BRCA2–RAD51 reactions, the diluted samples, as above, were incubated at 37°C in the absence or presence of 250 nM RAD51 for 30 min without shaking.

SFM imaging. Samples for SFM imaging were prepared by depositing 20 μl reaction on a freshly cleaved mica (Muscovite mica, V5 quality, EMS) for 2 min, followed by a 2 ml wash using 18 MΩ water and drying in filtered (0.22 μm) air. SFM images were scanned on a Nanoscope VIII scanner (Bruker), using tapping mode in air with a silicon probe, NHC-W, with tip radius <10 nm and resonance frequency range of 310–372 kHz (Nanosensor, Veeco Instruments, Europe). All images were acquired with a scan size of 2 × 2 μm at 512 × 512 pixels per image at 1 Hz. Images were processed using Nanoscope analysis (Bruker) for background flattening. Quantitative analyses of images was performed as described using SFMetrics software (27). Briefly, molecules from flattened SFM images were selected in the multimode image analysis mode of SFMetrics and thresholded to calculate volume, as the product of the average height and area. The molecular volume has been shown to linearly co-relate with the molecular mass of biomolecules in SFM height images (28). Thus, based on volume, the oligomeric state of the select molecule can be calculated. *Escherichia coli* RNA polymerase (RNAP), with a molecular mass of 450 kDa and volume of 678 nm^3, was used as a reference to determine the volume of one 2MBP-BRCA2 molecule (17). At 469 kDa, a monomer of 2MBP-fl-BRCA2 is equivalent to 1.04 RNAP or 707 nm^3. Volume less than half of monomer volume was used as a cut-off to threshold lower molecular mass species. Molecules with 0.5–1.5 monomer volume were designated

as monomer and so on. Monomer volume of each of the region was calculated similarly.

Volume of BRCA2–RAD51 complex depends on the organization of the complex and can be calculated assuming three possible arrangements. (i) Additive volume, if RAD51 molecules dock on the surface of BRCA2, the resultant volume of the complex will be the volume of 1 BRCA2 + nRAD51. (ii) BRCA2 volume, if RAD51 occupies a void inside a large complex it will not contribute to the envelope volume measured by SFM and would thus be equivalent to BRCA2 volume. (iii) Range between BRCA2 volume and additive volume, if RAD51 interaction induces reorganization of BRCA2 then the volume of the complex can range between monomer volume of BRCA2 to the additive volume. In SFM experiments we observe a change in conformation of BRCA2 on interaction with RAD51 and thus scenario 3 is the closest assumption for BRCA2–RAD51 complex. Purified fl-BRCA2 binds 6 RAD51 monomers in conditions similar to those applied here (3). A BRCA2-RAD51 complex with one BRCA2 (707 nm^3) and six RAD51 ($56 \times 6 = 336$ nm^3) can have maximum volume of 1043 nm^3, which falls within the range of monomer volume for BRCA2 (353–1060 nm^3). Thus, in samples with BRCA2–RAD51 complex, monomer volume of BRCA2 was used for quantitation, with half monomer volume of BRCA2 as the threshold. For different regions of BRCA2 under study, using similar approach, monomer volume of BRCA2-region: nRAD51 complex can include one BRCA2 region with 2–5 RAD51 molecules (see Supplementary Table S1 for more details). Oligomeric volume of the different regions was calculated similarly. At 56 nm^3 the monomer volume of RAD51 is much lower than the threshold volume and thus free RAD51 is removed from analysis (Supplementary Figure S3).

The conformation of the molecules was quantified by the parameters of solidity. Solidity is the ratio of the area of an object to the area of a convex hull that completely encloses the object. Solidity in a scale of 1 to 0 quantifies the globularity ($S \sim 1$) and irregularity ($S \sim 0$) of a molecular shape. Change in solidity provides a quantitative readout for change in the shape of a molecule and is independent of its size.

RESULTS

To determine which parts of BRCA2 contribute to the observed conformational flexibility *in vitro*, we cloned, expressed and purified five regions of BRCA2 (Figure 1A and Supplementary Figure S1). Three regions, N-terminal (N: aa 1–939), Brc Repeat region (R: aa 940–2130) and C-terminal (C: aa 2131–3418), which span the length of the protein without sequence overlap. Two regions, N-terminal-Repeat region (NR: aa 1–2130) and Brc Repeat region-C-terminal (RC: aa 940–3418) both include the Brc repeat region in combination with either the N- or C-terminus, each representing about two thirds of the full-length protein. We analysed the different regions for their probability of intrinsic disorder with respect to fl-BRCA2 using web-based tool IUPred2A. All the regions exhibited similar profile for intrinsic disorder, as fl-BRCA2, suggesting suboptimal prediction of changes that are likely to arise due to deletion of parts of BRCA2 (Supplementary Figure S4).

In single molecule conformation studies, we define molecular architecture of BRCA2 assemblies with the parameters: oligomerization and solidity. Oligomerization is determined by volumetric analysis, in which measured volume and expected volume of a monomeric unit are used to compute the oligomeric state of the molecule. Solidity quantifies the shape of the molecule in a spectrum of globular (with solidity ∼1) to highly irregular (with solidity ∼0). The conformational landscape is represented in the distribution of these forms in a population and changes in the distribution.

Flexibility is most prominent for BRCA2 N- and C-terminal regions

Purified proteins were imaged after incubation at 37 and 0°C and the images were analysed for oligomerization and solidity (17,27). In SFM images, all the proteins appeared as complexes of irregular size at 37°C with fl-BRCA2 also showing irregularity in shape with prominent extensions (Figure 2A: 37°C). BRCA2 molecules incubated at 0°C, before deposition, were more compact and globular (Figure 2A: fl-BRCA2 panel). The distribution of molecules with varying solidity showed a definitive shift towards higher solidity (∼0.9) *i.e.*, more globular at lower temperature (37 versus 0°C) (Figure 2B: fl-BRCA2 panel). Similar to fl-BRCA2, all the regions including the N- or C-terminus (N, C, NR and RC) changed conformation with temperature (Figure 2A, B). The R region alone did not change in conformation with temperature (Figure 2A, B: panels labelled R). RC like fl-BRCA2 was more compact (distribution shifting toward higher solidity) at lower temperature (0°C) while the N, C and NR became more extended and irregular (distribution shifted toward lower solidity) (Figure 2B). This opposite change in molecular conformation in different regions with temperature, is likely a complex phenomenon, which has been observed in earlier temperature dependent studies in disordered proteins but is not fully understood (29–31).

The distribution of oligomeric states for fl-BRCA2 and the RC region did not change with temperature, suggesting that the same size complex became more compact (Figure 2C and Supplementary Table S2). This more compact conformation for fl-BRCA2 and RC likely represents lower conformational entropy at 0°C (32,33). Correspondingly, the absence of change in distribution of forms in the R region (Figure 2B and C and Supplementary Table S2) indicates low flexibility, more ordered structure, including inter/intra-molecular interactions among the eight Brc repeats that consequently allow less freedom to move. Increased irregularity of N and C regions, was accompanied by higher oligomerization at lower temperatures (Figure 2C and Supplementary Table S2), signifying that low temperature favours conformations that promoted oligomerization. The NR variant was more irregular at lower temperatures together with a slight decrease in larger oligomeric forms and an increase in the dimer, trimer and tetramer popula-

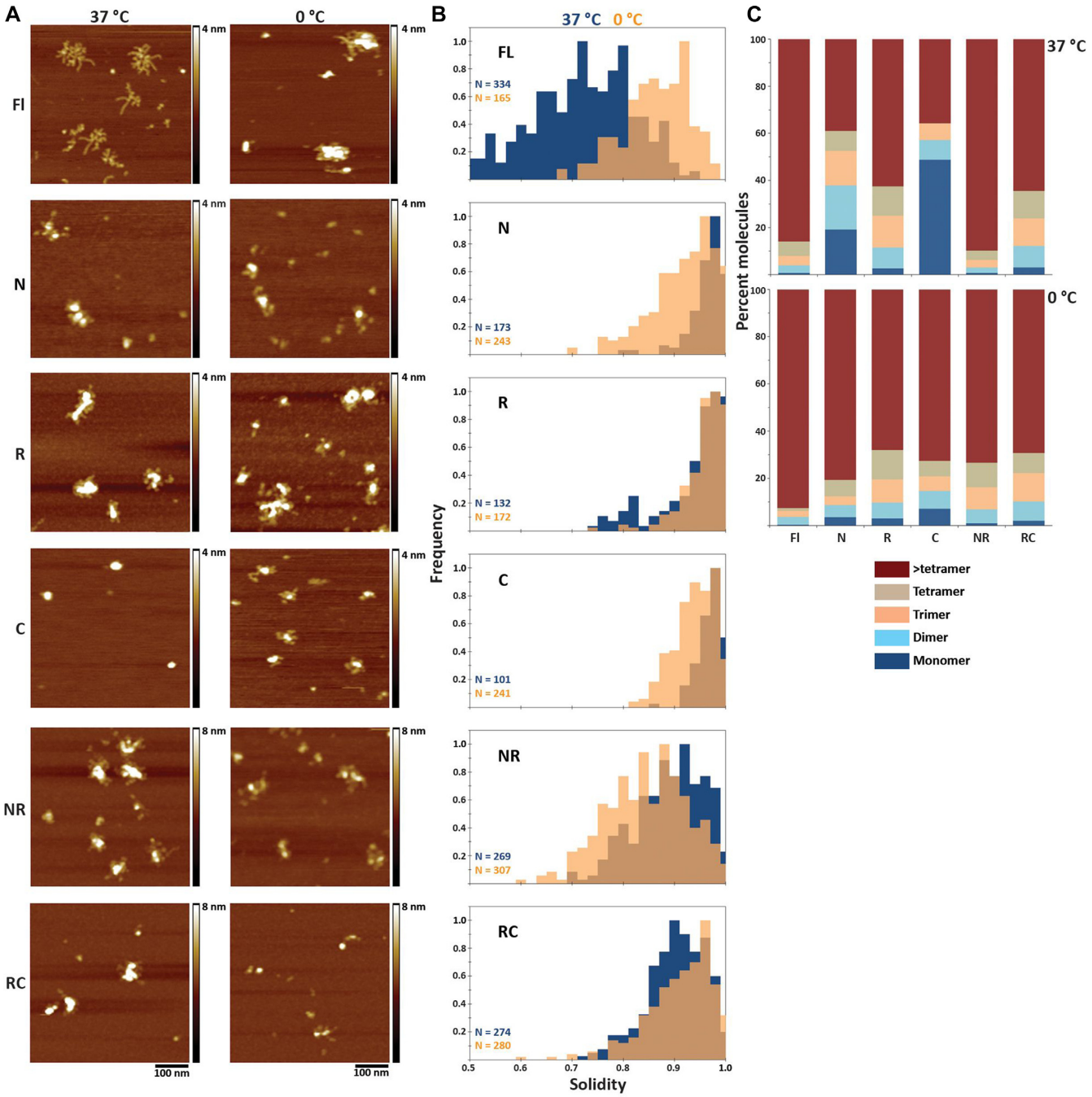

Figure 2. The N- and C-terminal regions of BRCA2 provide flexibility to fl-BRCA2. (**A**) Representative SFM height images showing change in conformation of fl-BRCA2 and the different regions at 37 and 0°C. The representative images do not necessarily depict the most populous molecular assemblies but are aimed to show, as much as is possible in a single image, the range of architecture of BRCA2 constructs. Note: The *Z*-scale in some of the images is different to allow optimal visualization of molecules. (**B**) Histograms showing change in solidity, readout for conformational flexibility, of the BRCA2 regions with temperature, at 37 and 0°C. Histograms for solidity were normalised to their maximum value. (**C**) Oligomeric distribution of the BRCA2 regions at 37 and 0°C.

tion (Figure 2B and C, Supplementary Table S2). All proteins including the N region (N, NR and fl-BRCA2) showed a change in conformation with temperature and a relatively broad spread in conformational distribution (Figure 2B: solidity) indicating that the N region is the most flexible part of BRCA2, followed by the C region.

All regions of BRCA2 can interact with RAD51

Extended fl-BRCA2 adopts a characteristic compact and elongated conformation on interaction with RAD51 (17). These compact assemblies, formed at a molar ratio of 1:24 (BRCA2:RAD51) and cross-linked by glutaraldehyde, were highly oligomeric with 12–26 BRCA2 molecules and 50–100

RAD51 molecules per complex (17). To dissect the contribution of different regions of BRCA2 to this transition we determined the effect of RAD51 on conformational landscape of the five BRCA2 regions (N, R, C, NR and RC). In order to reveal the multimeric state of the different regions we did not fix the samples with glutaraldehyde in the present study. In the absence of RAD51, 68% of the fl-BRCA2 was present in irregular, oligomeric assemblies, whose volume indicated complexes larger than tetramers (Figure 3A and B, Supplementary Table S3). Fl-BRCA2 reorganized in the presence of RAD51 into predominantly monomeric complexes (75%) with compact conformation (Figure 3B and C: fl-BRCA2+RAD51 and Supplementary Table S3).

Among the different regions, the isolated N (42%) and C (41%) regions had the smallest percentage of larger oligomers (Figure 3B, Supplementary Figure S5 and Supplementary Table S3). BRCA2 parts including the R region, R (59%), NR (74%) and RC (66%), showed most oligomeric complexes in the size range larger than tetramers. On incubation with RAD51, oligomers diminished and the population shifted to majority monomer to dimer, N (90%), C (63%) and NR (95%) (percent molecules here = monomers + dimers) (monomer volume of BRCA2-region: nRAD51 complex includes 1 BRCA2 region with 2–5 RAD51 molecules: for details see materials and methods: SFM imaging) (Figure 3, Supplementary Figure S5 and Supplementary Table S3). The R region also showed a decrease in large oligomers (37 *vs* 59%) accompanied by molecules reorganizing into tetramers (13%), trimers (20%) and dimers (20%). The RC region showed the smallest change in oligomerization with only ∼10% of large oligomers shifted towards smaller assemblies (Figure 3, Supplementary Figure S5 and Supplementary Table S3). However, average solidity of RC complexes changed the most from ∼0.9 to ∼1 on interaction with RAD51 (Figure 3C: RC). Thus, the RC region did rearrange most likely from BRCA2–BRCA2 oligomers to BRCA2–RAD51 oligomers. In all the cases, incubation with RAD51 caused an increase in monomer/dimer sized complexes and decrease in complexes larger than tetramers (Figure 3B).

Brc repeats behave differently in isolation versus as part of BRCA2

Biochemically the eight Brc repeats are reported to have different affinities for RAD51 and function in two modules of Brc 1–4 and Brc 5–8 (7,11). To determine the contribution of these two modules of Brc repeats to oligomerization and conformation of fl-BRCA2 we prepared regions with deletion of Brc 1–4 (BRCA2 ΔBrc 1–4, Δaa 940–1549) and Brc 5–8 (BRCA2 ΔBrc 5–8, Δaa 1665–2130) along with complementary fragments consisting only of the repeat regions of Brc 1–4 (aa 940–1664) and Brc 5–8 (aa 1550–2130) (Figure 1A). These regions were incubated in the presence or absence of RAD51 and analysed for oligomerization (17,27). Monomer volume of BRCA2-region:nRAD51 complex includes one BRCA2 region with 2–5 RAD51 molecules (for details, see Materials and Methods: SFM imaging).

BRCA2 ΔBrc 1–4 appeared as irregular multimeric assemblies with 79% of the molecules observed in clusters larger than tetramers, similar to fl-BRCA2. Whereas BRCA2 ΔBrc 5–8, although also irregular, formed fewer large oligomers with only 41% of complexes larger than tetramers. In isolation Brc 5–8 was also predominantly present as irregular multimeric assemblies, with 65% in oligomers larger than tetramers, thus being similar to BRCA2 ΔBrc 1–4 (Figure 4 and Supplementary Table S4). For both BRCA2 ΔBrc 5–8 and Brc 1–4, a higher proportion of the molecules were present in monomers. Therefore, whether in isolation or in the background of the rest of BRCA2, Brc 5–8 had a higher propensity to oligomerize (Figure 4B; no RAD51 panel, S6 and Supplementary Table S4).

On incubation with RAD51, all the Brc fragments formed compact elongated structures (Figure 4A and Supplementary Figure S7). Monomeric forms became the most prominent species for both BRCA2 ΔBrc 1-4-RAD51 (41%) and BRCA2 ΔBrc 5-8-RAD51 (63%) (Figure 4B and Supplementary Table S4). The isolated Brc repeats behaved differently. In the presence of RAD51, Brc 1–4 became predominantly dimer-trimer (25%, 22%) with loss of both monomers and large oligomers. Even in the presence of RAD51 the most prominent form of Brc 5–8 was large oligomers (39%). (Figure 4B and Supplementary Table S4). This observation differs from distribution of molecules without RAD51, where the major population in all the constructs was oligomers larger than tetramers. BRCA2 ΔBrc 1–4 and BRCA2 ΔBrc 5–8 changed the most from large assemblies to monomers. The Brc 1–4 and Brc 5–8 showed reorganization into dimers, trimers and tetramers. Therefore, on interaction with RAD51, the modules of Brc repeats contribute to the oligomeric distribution differently. In isolation they are more multimeric while in the BRCA2 protein they promote monomeric assemblies, as for fl-BRCA2. Hence signifying that the contribution to conformational transitions and oligomerization of the two Brc modules is not independent but likely synergistic in the fl-BRCA2.

Single amino acid variation in F1524V alters conformational landscape of BRCA2

Fragments covering relatively large regions of $BRCA2^{wt}$ indicated their different contribution to the conformational landscape of the protein. We were curious if any of the single amino acid variants of unknown significance (VUS, often reported from breast cancer patient derived sequencing studies, UniProtKB-P51587, BRCA2_HUMAN) could influence this conformational landscape. We screened a number of clinically relevant variants of BRCA2 and selected two, F1524V and G1771D to probe their functional significance in detail. The variations lie in the Brc repeat region and were identified in genetic screens from breast cancer patients (34,35). The choice of these variants was based on two criteria, 1) the amino acid change is in the RAD51 interacting region of Brc repeats, and 2) the variation is likely to perturb innate interactions of the $BRCA2^{wt}$. In $BRCA2^{F1524V}$, the hydrophobic phenylalanine is replaced by an aliphatic valine, predicted to destabilize Brc4-RAD51 interaction (36) and possibly altering a structural motif due to different spatial geometry. In $BRCA2^{G1771D}$, a small aliphatic glycine is replaced by negatively charged bulkier glutamate likely resulting in gain of electrostatic interaction

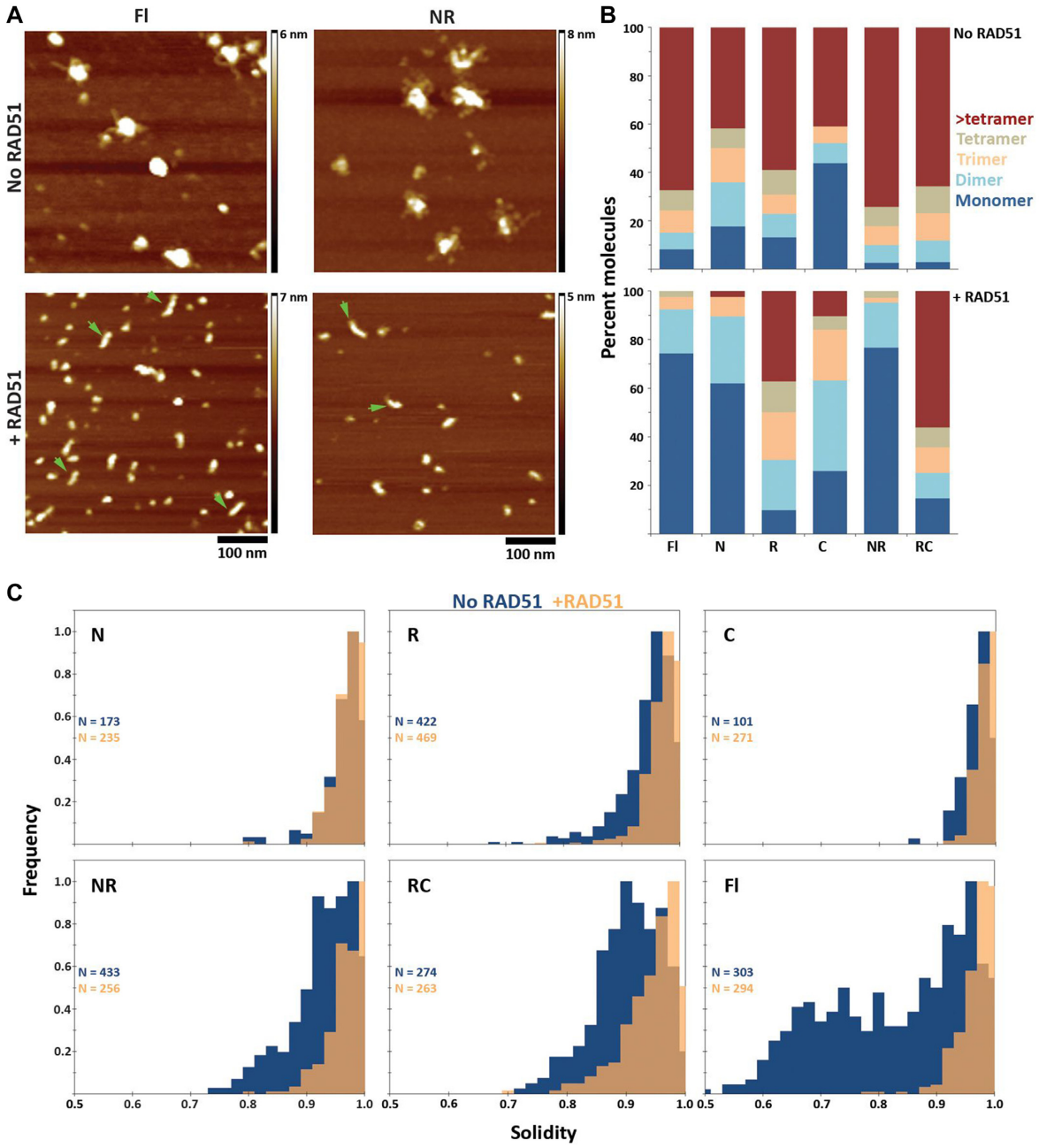

Figure 3. All regions of BRCA2 interact with RAD51. (**A**) Representative SFM height images showing change in conformation of fl-BRCA2 and NR region in the presence of RAD51, 37°C. Green arrows highlight compact elongated assemblies in the presence of RAD51. The representative images do not necessarily depict the most populous molecular assemblies but are aimed to show, as much as is possible in a single image, the range of architecture of BRCA2 constructs. Note: The Z-scale in the images is different to allow optimal visualization of molecules. (**B**) Oligomeric distribution and (**C**) histogram showing distribution of conformations for fl, N, R, C, NR, RC regions in the absence and presence of RAD51. Histograms for solidity were normalised to their maximum value. Differences in conformation of fl-BRCA2 and regions between Figure 2 (37°C) and Figure 3 (no RAD51) reflects variation between protein preparation from plate and suspension culture and the corresponding yields (see Supplementary Figure S6 and accompanying note).

or steric hindrance. The variants were imaged in the presence and absence of RAD51 and analysed for oligomerization and solidity.

Both the single amino acid variants, like BRCA2^{wt}, formed irregular multimeric assemblies (Figures 3A, 5A and Supplementary Figure S8). In the absence of RAD51, BRCA2^{F1524V} and BRCA2^{G1771D} were similar to BRCA2^{wt} with extended shape and average solidity at ∼0.8 (Figure 5C and Supplementary Table S5). With respect to oligomerization, BRCA2^{F1524V} deviated the most, consisting of only 35% oligomers larger than tetramers versus 68% for BRCA2^{wt} and 63% for BRCA2^{G1771D} (Figures 5B, Supplementary Figure S8 and Supplementary Table S6). Moreover, the BRCA2^{F1524V} variant had the highest proportion of monomers at 28%, signifying a reduced ability to self-associate (Figure 5B and Supplementary Table S6).

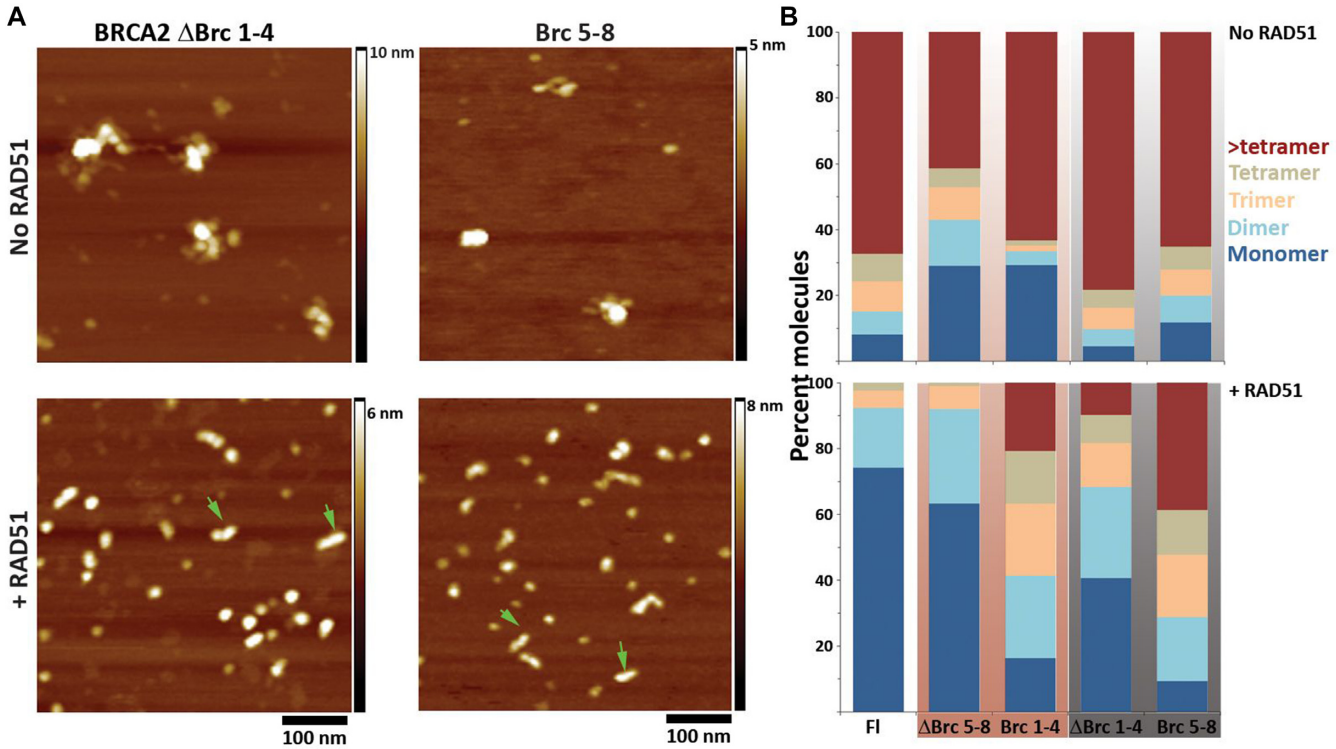

Figure 4. Brc repeats of BRCA2 contribute synergistically to the conformational landscape of the full-length protein. (**A**) Representative SFM height images of BRCA2 ΔBrc 1–4 (left panel) and Brc 5–8 (right panel) in the absence and presence of RAD51. Green arrows highlight compact elongated assemblies in the presence of RAD51. The representative images do not necessarily depict the most populous molecular assemblies but are aimed to show, as much as is possible in a single image, the range of architecture of BRCA2 constructs. Note: The Z-scale in the images is different to allow optimal visualization of molecules. (**B**) Oligomeric distribution of fl, BRCA2 ΔBrc 5–8, Brc 1–4, BRCA2 ΔBrc 1–4 and Brc 5–8 in the absence (top panel) and presence (bottom) of RAD51. Brc 1–4 and Brc 5–8 are controls for BRCA2 ΔBrc 5–8 and BRCA2 ΔBrc 1–4, respectively. Distinct oligomeric profiles of the two groups, highlighted in red and grey rectangles, on interaction with RAD51 show that Brc 1–4 and Brc 5–8 are biochemically distinct in isolation.

The most notable conformational change of $BRCA2^{wt}$ in our studies was upon interaction with RAD51. Particularly, the large oligomers of BRCA2 reorganized into prominent monomer population in the presence of RAD51. This change was evident in $BRCA2^{G1771D}$, where the distribution of forms was similar to $BRCA2^{wt}$ where larger oligomers diminished to redistribute mostly in monomers, dimers and trimers. $BRCA2^{F1524V}$ however, showed almost no change in oligomeric distribution in response to RAD51 (Figure 5B and Supplementary Table S6).

The conformational distribution for $BRCA2^{G1771D}$ was similar to $BRCA2^{wt}$, with average solidity of ∼1 in the presence of RAD51. For $BRCA2^{F1524V}$, although volume distribution did not change, there was a change in conformation upon interacting with RAD51. This conformational change however was also muted, compared to $BRCA2^{wt}$ and $BRCA2^{G1771D}$, displaying an average solidity of ∼0.9 upon incubation with RAD51 (Figures 5A, Supplementary Figure S8 and Supplementary Table S5). For $BRCA2^{F1524V}$ about 30% of the molecules had solidity <0.9 while in $BRCA2^{wt}$ and $BRCA2^{G1771D}$ this was a negligible percentage, 1%, and 4% respectively. A notable number of $BRCA2^{F1524V}$ molecules in SFM images also displayed an extended conformation revealing lack of conformational change upon interaction with RAD51 (Figure 5A). The single amino acid change in the variant F1524V had a large influence (equivalent to or greater than deleting a region including Brc 1–4) on both self-oligomers of BRCA2 and an impaired conformational switch on interaction with RAD51.

DISCUSSION

To understand how different parts of BRCA2 contribute to its flexibility we prepared regions of BRCA2 and systematically quantified their conformational profile with respect to solidity and oligomerization. Temperature induced changes in the different regions, at 37 and 0°C, indicated plasticity and identified the N and C regions of BRCA2 as most flexible. All regions including either N- or C-terminal part (N, C, NR and RC) changed conformation with temperature. The temperature induced change in solidity distribution among the smaller regions (N, C, NR and RC) was not as prominent as for fl-BRCA2, probably due to their smaller size, which were not as irregular or extended to begin with. The observed low oligomerization of the N and C region along with highly oligomeric assemblies of segments including the R region is indicative of the importance of Brc repeat region in BRCA2–BRCA2 interaction. The R region did not show any temperature induced change. However, NR and RC did change despite the presence of the Brc repeats demonstrating that the flexible N- and C-terminal regions can influence Brc repeat mediated self-oligomerization of BRCA2. Each region, N, R and C, exhibited plasticity in different

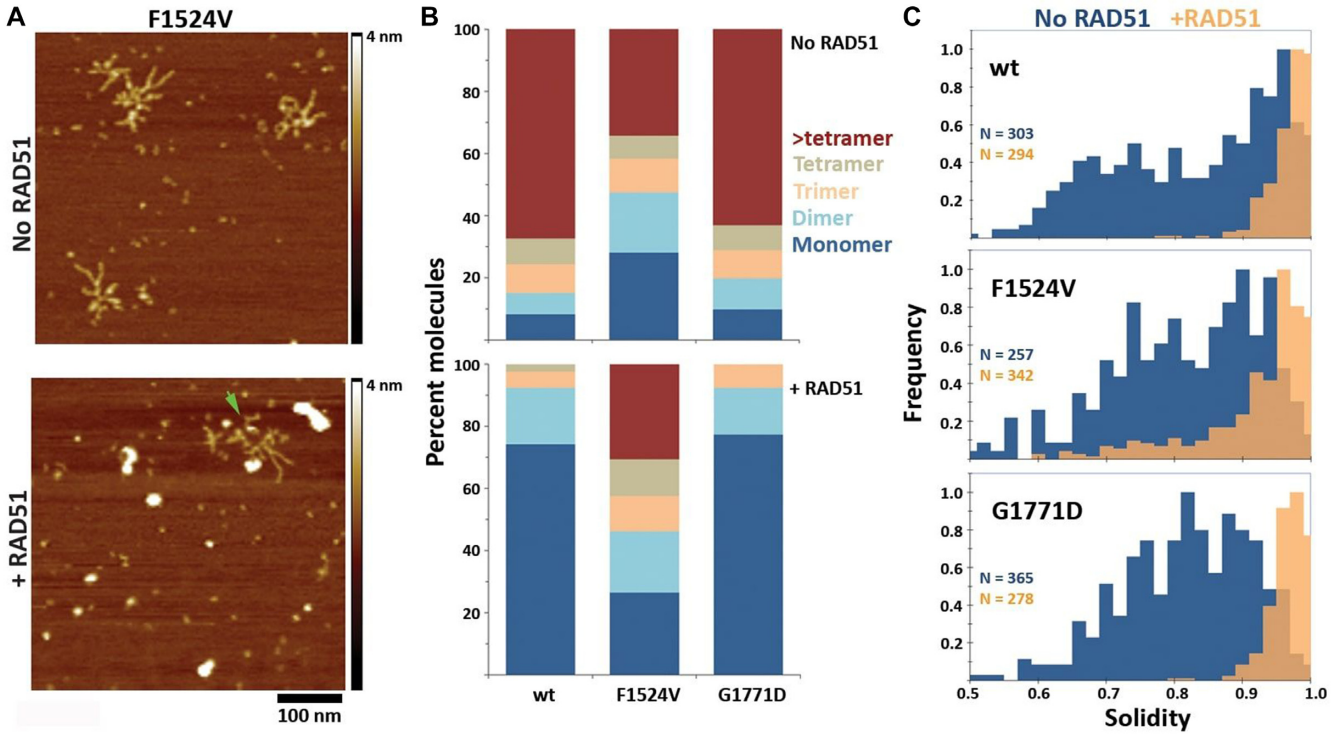

Figure 5. Single amino acid variations in BRCA2^{wt} can alter conformational landscape of the protein. (**A**) Representative SFM height image of BRCA2^{F1524V} in the absence (top panel) and presence (bottom panel) of RAD51. Green arrow highlights the persistence of flexible extended molecules in the presence of RAD51. The representative images do not necessarily depict the most populous molecular assemblies but are aimed to show, as much as is possible in a single image, the range of architecture of BRCA2 constructs. (**B**) Oligomeric distribution and (**C**) histogram of conformation for wt, F1524V and G1771D in the absence and presence of RAD51. Histograms for solidity were normalised to their maximum value.

ways compared to the complete protein demonstrating interdependence of different regions of BRCA2 for its overall conformation.

Segments including the N region (fl, N, NR) became predominantly monomeric on interaction with RAD51 while C region showed a peak population at monomers and dimers. Therefore, C region also appears to be involved in oligomerization, as indicated by prominent dimers + trimers in C-RAD51 reactions, while N appears to promote monomerization. The observations of change in self-oligomeric state of BRCA2 on incubation with a binding partner is in agreement with a recent report, where self-association of BRCA2 *via* the N and C regions was shown to be sensitive to BRCA2 interacting partners, DSS1 and ssDNA (25). The R and RC regions even in the presence of RAD51 were mostly larger oligomers, reaffirming the role of the R region in oligomerization. The discrete pattern of interaction of different regions of BRCA2 on interaction with RAD51 is suggestive of specific functional role, most likely either in a cascade of reactions or *via* dynamic allostery (2,37,38).

The two Brc modules, Brc 5–8 and Brc 1–4, also had distinct oligomeric profiles in the presence of RAD51. These modules are biochemically different with respect to their potential for free RAD51 binding, inhibition of DNA-dependent ATPase activity of RAD51 and RAD51 mediated DNA strand exchange reaction (7,11). Data from GST pull-down assays by Carreira *et al.* indicate very weak affinity of Brc 5–8, in the range of 100–200 μM, for free RAD51 (7). We observed here that Brc 5–8 reproducibly showed significant reorganization in the presence of RAD51, suggesting that RAD51 induced reorganization of BRCA2 oligomers does not require very strong affinity. Deletion of either repeat module, for example in BRCA2 ΔBrc 1–4 which retains the Brc 5–8 module, resulted in a protein with oligomeric forms more like fl-BRCA2–RAD51 than like Brc 5-8-RAD51. In the context of fl-BRCA2, the behaviour of Brc 1–4 and Brc 5–8 is not the sum of their behaviour in isolation but rather they exhibit synergistic behaviour, a characteristic of IDPs, where different parts of a protein cross-talk to define the conformational landscape of the whole molecule.

In addition to the R region, the N and the C region also show conformational transition on incubation with RAD51. While there is a reported phosphorylation dependent binding site for RAD51 in the C-terminal region (15), the N-terminal regions is not known to interact with RAD51 (11). The eight Brc repeats have highly conserved tetra amino acid motifs of FxxA, FxxG and xFxE that are reported to be key for RAD51 interaction (10,14). A sequence search of BRCA2 for potential FxxA, FxxG and xFxE motifs revealed that the N- and the C-terminal region also have a number of these potential RAD51 interaction motifs (Supplementary Table S7). However, being very short motifs, only four amino acids, they are likely to be degenerate and their mere presence is not sufficient to explain the observed conformational changes. Further systematic conformational and biochemical experiments are needed to elucidate the nature of N region and RAD51 interaction.

For more specific information on BRCA2 conformational flexibility we analysed two clinically identified variants of BRCA2, BRCA2^{F1524V}, BRCA2^{G1771D}, both located in the Brc repeats (34,35). The single amino acid change BRCA2^{F1524V}, in the Brc 4 repeat, drastically impaired the characteristic conformational change of BRCA2 on interaction with RAD51. More than a third of molecules analysed failed to adopt a compact conformation and retained the flexible extended conformation. The residue F1524 is the phenylalanine of the FxxA motif of Brc 4 and mutation of phenylalanine at 1524 to valine, most likely disrupts hydrophobic interaction with RAD51 (9). This suggests that interaction with RAD51 and the Brc 4 is crucial for the dynamic allosteric interactions resulting in the compact BRCA2-RAD51 conformation. The observed variety of conformations is indicative of multiple energetically equivalent conformations in BRCA2, one or more of which is not able to interact with RAD51 when phenylalanine 1524 is replaced by a valine.

Given that all the regions of BRCA2 can interact with RAD51 and undergo a conformational change, it is intriguing to speculate how these interactions could contribute to BRCA2 function. Multivalent interaction of BRCA2 with RAD51 may be spatio-temporally decoupled such that they contribute to different functions of BRCA2. Distinct functional profiles of the Brc–RAD51 interaction and CDK1/2 phosphorylation dependent interaction of the C-terminal RAD51 binding site at S3291 have been suggested previously (10–12,15,16,39). Broadly, while interaction with the Brc repeats allows BRCA2 to carry RAD51 to the site of DNA damage, the C-terminal interaction appears to be regulatory in nature. It is thus likely that the N-terminal interactions are also modulatory in function, conditions of which need to be explored further.

BRCA2 is a complex protein comprising multiple IDRs interspersed throughout 3418 aa. Proteins with significant amounts of IDRs are characterized by flexible backbones that allow sampling numerous energetically equivalent conformations, thereby giving rise to an ensemble of functionally competent conformations. Multi-valency coupled with dynamic allostery can function as a dynamic switch, in response to micro-environment changes and interacting partners, to orchestrate complex molecular functions without needing high energy co-factors (2,37,40–44). BRCA2 is a hub for interactions among proteins involved in homologous recombination, in the centre of a dynamic functional landscape. Here, we begin to define BRCA2's conformational landscape, as a step to determine how this facilitates essential molecular hand-off reactions in genome maintenance.

SUPPLEMENTARY DATA

Supplementary Data are available at NAR Online.

ACKNOWLEDGEMENTS

We thank. R. Kanaar and J. Lebbink for discussions and comments on the manuscript.

FUNDING

Dutch Cancer Society project [KWF 10436 to C.W.]; Gravitation program CancerGenomiCs.nl from the Netherlands Organisation for Scientific Research (NWO) and is part of the Oncode Institute, which is partly financed by the Dutch Cancer Society; Dutch Technology Foundation (STW) project [NWOnano11425 to C.W.]; Marie Curie Reintegration Grant [FP7-276898 to H.S.]. The open access publication charge for this paper has been waived by Oxford University Press – *NAR* Editorial Board members are entitled to one free paper per year in recognition of their work on behalf of the journal.
Conflict of interest statement. None declared.

REFERENCES

1. Iakoucheva,L.M., Brown,C.J., Lawson,J.D., Obradovic,Z. and Dunker,A.K. (2002) Intrinsic disorder in cell-signaling and cancer-associated proteins. *J. Mol. Biol.*, **323**, 573–584.
2. Dunker,A.K., Brown,C.J., Lawson,J.D., Iakoucheva,L.M. and Obradovic,Z. (2002) Intrinsic disorder and protein function. *Biochemistry*, **41**, 6573–6582.
3. Jensen,R.B., Carreira,A. and Kowalczykowski,S.C. (2010) Purified human BRCA2 stimulates RAD51-mediated recombination. *Nature*, **467**, 678–683.
4. Holloman,W.K. (2011) Unraveling the mechanism of BRCA2 in homologous recombination. *Nat. Struct. Mol. Biol.*, **18**, 748–754.
5. Liu,J., Doty,T., Gibson,B. and Heyer,W.D. (2010) Human BRCA2 protein promotes RAD51 filament formation on RPA-covered single-stranded DNA. *Nat. Struct. Mol. Biol.*, **17**, 1260–1262.
6. Thorslund,T., McIlwraith,M.J., Compton,S.A., Lekomtsev,S., Petronczki,M., Griffith,J.D. and West,S.C. (2010) The breast cancer tumor suppressor BRCA2 promotes the specific targeting of RAD51 to single-stranded DNA. *Nat. Struct. Mol. Biol.*, **17**, 1263–1265.
7. Carreira,A. and Kowalczykowski,S.C. (2011) Two classes of BRC repeats in BRCA2 promote RAD51 nucleoprotein filament function by distinct mechanisms. *Proc. Natl. Acad. Sci. U.S.A.*, **108**, 10448–10453.
8. Bork,P., Blomberg,N. and Nilges,M. (1996) Internal repeats in the BRCA2 protein sequence. *Nat. Genet.*, **13**, 22–23.
9. Pellegrini,L., Yu,D.S., Lo,T., Anand,S., Lee,M., Blundell,T.L. and Venkitaraman,A.R. (2002) Insights into DNA recombination from the structure of a RAD51-BRCA2 complex. *Nature*, **420**, 287–293.
10. Rajendra,E. and Venkitaraman,A.R. (2010) Two modules in the BRC repeats of BRCA2 mediate structural and functional interactions with the RAD51 recombinase. *Nucleic Acids Res.*, **38**, 82–96.
11. Chatterjee,G., Jimenez-Sainz,J., Presti,T., Nguyen,T. and Jensen,R.B. (2016) Distinct binding of BRCA2 BRC repeats to RAD51 generates differential DNA damage sensitivity. *Nucleic Acids Res.*, **44**, 5256–5270.
12. Martinez,J.S., von Nicolai,C., Kim,T., Ehlen,A., Mazin,A.V., Kowalczykowski,S.C. and Carreira,A. (2016) BRCA2 regulates DMC1-mediated recombination through the BRC repeats. *Proc. Natl. Acad. Sci. U.S.A.*, **113**, 3515–3520.
13. Wong,A.K., Pero,R., Ormonde,P.A., Tavtigian,S.V. and Bartel,P.L. (1997) RAD51 interacts with the evolutionarily conserved BRC motifs in the human breast cancer susceptibility gene brca2. *J. Biol. Chem.*, **272**, 31941–31944.
14. Lo,T., Pellegrini,L., Venkitaraman,A.R. and Blundell,T.L. (2003) Sequence fingerprints in BRCA2 and RAD51: implications for DNA repair and cancer. *DNA Repair (Amst.)*, **2**, 1015–1028.
15. Esashi,F., Christ,N., Gannon,J., Liu,Y., Hunt,T., Jasin,M. and West,S.C. (2005) CDK-dependent phosphorylation of BRCA2 as a regulatory mechanism for recombinational repair. *Nature*, **434**, 598–604.
16. Ayoub,N., Rajendra,E., Su,X., Jeyasekharan,A.D., Mahen,R. and Venkitaraman,A.R. (2009) The carboxyl terminus of Brca2 links the disassembly of Rad51 complexes to mitotic entry. *Curr. Biol.*, **19**, 1075–1085.

17. Sanchez,H., Paul,M.W., Grosbart,M., van Rossum-Fikkert,S.E., Lebbink,J.H.G., Kanaar,R., Houtsmuller,A.B. and Wyman,C. (2017) Architectural plasticity of human BRCA2-RAD51 complexes in DNA break repair. *Nucleic Acids Res.*, **45**, 4507–4518.
18. Oliver,A.W., Swift,S., Lord,C.J., Ashworth,A. and Pearl,L.H. (2009) Structural basis for recruitment of BRCA2 by PALB2. *EMBO Rep.*, **10**, 990–996.
19. Yang,H., Jeffrey,P.D., Miller,J., Kinnucan,E., Sun,Y., Thoma,N.H., Zheng,N., Chen,P.L., Lee,W.H. and Pavletich,N.P. (2002) BRCA2 function in DNA binding and recombination from a BRCA2-DSS1-ssDNA structure. *Science*, **297**, 1837–1848.
20. van der Heijden,T., Seidel,R., Modesti,M., Kanaar,R., Wyman,C. and Dekker,C. (2007) Real-time assembly and disassembly of human RAD51 filaments on individual DNA molecules. *Nucleic Acids Res.*, **35**, 5646–5657.
21. Modesti,M., Ristic,D., van der Heijden,T., Dekker,C., van Mameren,J., Peterman,E.J., Wuite,G.J., Kanaar,R. and Wyman,C. (2007) Fluorescent human RAD51 reveals multiple nucleation sites and filament segments tightly associated along a single DNA molecule. *Structure*, **15**, 599–609.
22. Sanchez,H., Kertokalio,A., van Rossum-Fikkert,S., Kanaar,R. and Wyman,C. (2013) Combined optical and topographic imaging reveals different arrangements of human RAD54 with presynaptic and postsynaptic RAD51-DNA filaments. *Proc. Natl. Acad. Sci. U.S.A.*, **110**, 11385–11390.
23. Shahid,T., Soroka,J., Kong,E., Malivert,L., McIlwraith,M.J., Pape,T., West,S.C. and Zhang,X. (2014) Structure and mechanism of action of the BRCA2 breast cancer tumor suppressor. *Nat. Struct. Mol. Biol.*, **21**, 962–968.
24. Braga,P.C. and Ricci,D. (2004) In: *Atomic Force Microscopy: Biomedical Methods and Applications*. Humana Press, NY.
25. Le,H.P., Ma,X., Vaquero,J., Brinkmeyer,M., Guo,F., Heyer,W.D. and Liu,J. (2020) DSS1 and ssDNA regulate oligomerization of BRCA2. *Nucleic Acids Res*., doi:10.1093/nar/gkaa555.
26. Babu,M.M., Kriwacki,R.W. and Pappu,R.V. (2012) Structural biology. Versatility from protein disorder. *Science*, **337**, 1460–1461.
27. Sanchez,H. and Wyman,C. (2015) SFMetrics: an analysis tool for scanning force microscopy images of biomolecules. *BMC Bioinformatics*, **16**, 27.
28. Ratcliff,G.C. and Erie,D.A. (2001) A novel single-molecule study to determine protein–protein association constants. *J. Am. Chem. Soc.*, **123**, 5632–5635.
29. Wuttke,R., Hofmann,H., Nettels,D., Borgia,M.B., Mittal,J., Best,R.B. and Schuler,B. (2014) Temperature-dependent solvation modulates the dimensions of disordered proteins. *Proc. Natl. Acad. Sci. U.S.A.*, **111**, 5213–5218.
30. Kjaergaard,M., Norholm,A.B., Hendus-Altenburger,R., Pedersen,S.F., Poulsen,F.M. and Kragelund,B.B. (2010) Temperature-dependent structural changes in intrinsically disordered proteins: formation of alpha-helices or loss of polyproline II? *Protein Sci.*, **19**, 1555–1564.
31. Jephthah,S., Staby,L., Kragelund,B.B. and Skepo,M. (2019) Temperature dependence of intrinsically disordered proteins in dimulations: what are we missing? *J. Chem. Theory Comput.*, **15**, 2672–2683.
32. Dyson,H.J. and Wright,P.E. (1998) Equilibrium NMR studies of unfolded and partially folded proteins. *Nat. Struct. Biol.*, **5**, 499–503.
33. Fitter,J. (2003) A measure of conformational entropy change during thermal protein unfolding using neutron spectroscopy. *Biophys. J.*, **84**, 3924–3930.
34. Meyer,P., Voigtlaender,T., Bartram,C.R. and Klaes,R. (2003) Twenty-three novel BRCA1 and BRCA2 sequence alterations in breast and/or ovarian cancer families in Southern Germany. *Hum. Mutat.*, **22**, 259.
35. Hadjisavvas,A., Charalambous,E., Adamou,A., Christodoulou,C.G. and Kyriacou,K. (2003) BRCA2 germline mutations in Cypriot patients with familial breast/ovarian cancer. *Hum. Mutat.*, **21**, 171.
36. Doss,C.G. and Nagasundaram,N. (2014) An integrated in silico approach to analyze the involvement of single amino acid polymorphisms in FANCD1/BRCA2-PALB2 and FANCD1/BRCA2-RAD51 complex. *Cell Biochem. Biophys.*, **70**, 939–956.
37. Tompa,P. (2014) Multisteric regulation by structural disorder in modular signaling proteins: an extension of the concept of allostery. *Chem. Rev.*, **114**, 6715–6732.
38. Berlow,R.B., Dyson,H.J. and Wright,P.E. (2018) Expanding the paradigm: intrinsically disordered proteins and allosteric regulation. *J. Mol. Biol.*, **430**, 2309–2320.
39. Davies,O.R. and Pellegrini,L. (2007) Interaction with the BRCA2 C terminus protects RAD51-DNA filaments from disassembly by BRC repeats. *Nat. Struct. Mol. Biol.*, **14**, 475–483.
40. van der Lee,R., Buljan,M., Lang,B., Weatheritt,R.J., Daughdrill,G.W., Dunker,A.K., Fuxreiter,M., Gough,J., Gsponer,J., Jones,D.T. *et al.* (2014) Classification of intrinsically disordered regions and proteins. *Chem. Rev.*, **114**, 6589–6631.
41. Uversky,V.N. (2011) Intrinsically disordered proteins from A to Z. *Int. J. Biochem. Cell Biol.*, **43**, 1090–1103.
42. Dunker,A.K., Cortese,M.S., Romero,P., Iakoucheva,L.M. and Uversky,V.N. (2005) Flexible nets. The roles of intrinsic disorder in protein interaction networks. *FEBS J.*, **272**, 5129–5148.
43. Gunasekaran,K., Tsai,C.J., Kumar,S., Zanuy,D. and Nussinov,R. (2003) Extended disordered proteins: targeting function with less scaffold. *Trends Biochem. Sci.*, **28**, 81–85.
44. Boehr,D.D., Nussinov,R. and Wright,P.E. (2009) The role of dynamic conformational ensembles in biomolecular recognition. *Nat. Chem. Biol.*, **5**, 789–796.